Mansour Omar (Orcid ID: 0000-0002-8441-1469)

The characterisation of Pluronic P123 micelles in the presence of sunscreen agents

Pauline Ragu[a], Ketan Ruparelia[a], Diego Alba Venero[b] and Omar T. Mansour[a,*]

[a]Leicester School of Pharmacy, Faculty of Health and Life Sciences, De Montfort University, The Gateway, Leicester, Leicestershire LE1 9BH, UK. E-mail: omar.mansour@dmu.ac.uk

[b]ISIS Neutron and Muon Source, Science and Technology Facilities Council, Rutherford Appleton Laboratory, Didcot, Oxfordshire OX11 0QX, UK

This article has been accepted for publication and undergone full peer review but has not been through the copyediting, typesetting, pagination and proofreading process which may lead to differences between this version and the Version of Record. Please cite this article as doi: 10.1111/ics.12856

Abstract

OBJECTIVES The triblock copolymer Pluronic® is widely used in the personal care industry, including sun protection, for its film forming and solubilisation capabilities. In this study, the effect of three commonly used organic UV filters (ethylhexyl methoxycinnamate (EMC), ethylhexyl triazone (EHT) and avobenzone (AVB)) on the structure of Pluronic P123 micelles was investigated.

METHODS The Pluronic P123 micelle structure has been investigated using dynamic surface tension, nuclear magnetic resonance (NMR) and small-angle neutron scattering (SANS).

RESULTS Dynamic surface tension results show strong interactions between the UV filters and Pluronic® evident by sharp changes in the surface activity of the latter. The NMR results have revealed the creation of a hydrophobic microenvironment special to the Pluronic PPO core group in the presence of UV filters. Some interaction with the hydrophilic EO was also recorded, albeit weaker. This is further confirmed by SANS, where the Pluronic P123 micelles interacted with varying strengths with the UV filters, resulting in sharp changes in their size and shape.

CONCLUSIONS We have demonstrated the sensitivity of the Pluronic P123 micelles to the presence of various UVA/B filters. The micelles shape varied from spherical to cylindrical as the concentration and type of the UV filters were varied. These variations in the shape are expected to have a significant effect on the sun protection factor (SPF), as it affects the solubilisation of the UV filters within a formulation in addition to the formulations' rheological profile and film forming behaviour.

Keywords sunscreens, surfactants, emulsions, formulation/stability, delivery/vectorization/penetration, small-angle neutron scattering

This article has been accepted for publication and undergone full peer review but has not been through the copyediting, typesetting, pagination and proofreading process which may lead to differences between this version and the Version of Record. Please cite this article as doi: 10.1111/ics.12856

Résumé

OBJECTIFS : le copolymère tribloc Pluronic® est largement utilisé dans le domaine des soins personnels, notamment la protection solaire, pour ses capacités de formation de film et de solubilisation. Cette étude a permis d'étudier l'effet de trois filtres UV organiques couramment utilisés (éthylhexyl méthoxycinnamate [EMC], éthylhexyl triazone [EHT] et avobenzone [AVB]) sur la structure des micelles P123 Pluronic.

MÉTHODES : la structure de la micelle P123 Pluronic a été étudiée à l'aide d'une tension superficielle dynamique, d'une résonance magnétique nucléaire (RMN) et d'une diffusion de neutrons aux petits angles (DNPA).

RÉSULTATS : les résultats de la tension superficielle dynamique montrent de fortes interactions entre les filtres UV et Pluronic®, ce qui se traduit par de fortes variations de l'activité superficielle de ce dernier. Les résultats de la RMN ont montré la création d'un micro-environnement hydrophobe spécifique au groupe principal de l'OPP pluronique en présence de filtres UV. Une certaine interaction avec l'OE hydrophile a également été enregistrée, quoique plus faible. Ceci est confirmé par la DNPA, où les micelles P123 Pluronic ont interagi avec des forces variables avec les filtres UV, entraînant des changements importants dans leur taille et leur forme.

CONCLUSIONS : nous avons démontré la sensibilité des micelles P123 Pluronic à la présence de différents filtres UVA/B. La forme des micelles variait de sphérique à cylindrique en fonction de la concentration et du type de filtres UV. Ces variations de forme devraient avoir un effet significatif sur le facteur de protection solaire (SPF), car elles affectent la solubilisation des filtres UV dans une formulation, en plus du profil rhéologique et du comportement de formation de film des formulations.

1. Introduction

Sun protection formulations, also commonly known as sunscreens, are widely used in the personal care industry by consumers to protect against harmful UV radiations (280-400 nm) [1]. Prolonged exposure to these harmful radiations may result in acute or chronic effects on the skin, such as; erythema (sunburn), premature skin ageing and skin cancer [2],[3]. The rate of incidence of non-melanoma skin cancer has been on the rise in the recent years [4]. For example, in the UK, over 100,000 new cases of non-melanoma skin cancer are diagnosed every year [5]. It is therefore imperative that proper measures are in place to protect the skin against these harmful UV radiations. One of which, is the frequent and correct use of sunscreens.

Sunscreens comprise a range of active ingredients that act as UV filters, providing a balanced protection approach from both UVA and UVB radiations. Additionally, sunscreens also contain a wide range of inactive ingredients, such as sensory enhancers (silicones and powders), film formers (silicone-polyurethane based waxes, triblock copolymers), emollients (oils and esters) and emulsifiers (ionic or non-ionic).

Pluronic® copolymers are a group of triblock polymeric (non-ionic) surfactants made of polypropylene oxide (PPO) and polyethylene oxide (PEO) (PEO-PPO-PEO) [6]. They are highly surface active, non-toxic and are commonly deployed by different industries such as the pharmaceutical and cosmetics industry, for their solubilisation[7–9], emulsifier [10, 11] and film forming[12] properties. This amphiphilic nature allows the formation of various aggregates such as core-shell spherical micelles[8], rod-like micelles[9], and liquid lamellar crystals[13] depending on the temperature and their concentration.

Moreover, the presence of Pluronic® copolymers in many formulations including sunscreens in different concentrations affects the existence, nature and types of these aggregates. This is even further complicated in the presence of other ingredients which may result in competitive or synergistic interactions [14], affecting their critical micelle concentration (CMC) and eventually their aggregation behaviour. These changes would highly affect the feel of these formulations, and more importantly, the ‘accessibility’ of the UV filters in the formulation once they

are applied on the skin. For example, Hanson *et.al.* have investigated the effect of both the surfactant (emulsifier) concentration and type on the photostability of the UVA filter Avobenzone (AVB). Simple surfactants such as sodium dodecylsulfate (SDS), cetyl trimethylammonium bromide (CTAB), trimethylammonium bromide (TTAB) and sodium dodecylbenzenesulfonate (SDBS) were used by the authors to solubilise AVB in water [15]. They concluded that the samples containing SDS at concentrations higher than its critical micelle concentration (CMC) showed the best results in terms of AVB solubilisation and photostability, followed by the TTAB, SDBS and CTAB. This stronger performance by the SDS in comparison to the other surfactants was attributed to the partitioning of the UV filter within the SDS micelle palisade, allowing UV filter-water interactions, essential for photostability. These observations strongly show that the surfactant structure and micelle shape/size play a significant role in the photostability of UV filters, which will most certainly influence the formulation's SPF. Furthermore, the performance of sunscreens is highly dependent on the surface tension during the film formation phase, their distribution on the skin and their rheological profile, all of which would be sensitive to the emulsifier(s)' structure present in a formulation[16, 17]. The sensitivity of the SPF to the rheological properties of sunscreen lotions was also highlighted by Hanno *et.al.* where a range of commercially available surfactants were used. It was noted that varying the surfactant had a significant impact on the rheological profile of the formulations, affecting the formed film thickness and consequently the SPF [18], echoing the findings from Liu *et.al.* where the thickness of the film formed by sunscreen lotions has been shown to directly influence the SPF[19].

The solubilisation of hydrophobic molecules such as drugs, dyes and oils, by Pluronic® has been investigated before. Several fragrances were also solubilised in Pluronic® F127 by Grillo *et.al.* where the structure of the F127 micelles was explored by differential scanning calorimetry (DSC), small-angle X-ray scattering (SAXS) and small-angle neutron scattering (SANS) [20]. The authors concluded that the insertion of the fragrances into the Pluronic® micelles has introduced variable but sharp changes to the micelles' morphology. Han *et.al.* investigated the interactions between antimetabolites and Pluronic® L62 micelles using SANS where changes in the micelle core hydration level in the presence of the

antimetabolites had significant impact on the micelle size and the aggregation number [8]. Given the frequent use of Pluronic® in sun protection lotions and sprays, for example, F127 in *Kiehl's* Ultra Light Daily UV Defense SPF50+ lotion or F108 in *La Roche-Posay*'s Anthelios Age Correct SPF50+ lotion, a better understanding of the effect of UV filters on the Pluronic® aggregates morphology is needed, something we believe has not been attempted yet.

Based on these considerations, this study presents a detailed morphological analysis of the Pluronic® P123 (PEO_{20}-PPO_{70}-PEO_{20}) micelles in the presence of the UVA filter 3-(4-tert-Butylphenyl)-1-(4-methoxyphenyl)propane-1,3-dione (Avobenzone, AVB), and the UVB filters (a) 2-Ethylhexyl (2E)-3-(4-methoxyphenyl) prop-2-enoate (Octinoxate, EMC) and (b) 2,4,6-trianilino(*p*-carbo-2-ethylhexyl-1-oxy)-1,3,5-triazine, (Ethylhexyl triazone, EHT), Scheme 1, in ethanolic aqueous solutions. The use of ethanol as a cosolvent has been shown to improve the solubility of hydrophobic molecules[21], in addition to improving the feel of topical formulations intended for skin care[22]. We use dynamic surface tension (DST) to investigate the surface activity of P123 in the absence and the presence of the UV filters, nuclear magnetic resonance (NMR) to investigate any molecular interactions leading to structural changes, and lastly small-angle neutron scattering (SANS) to examine the morphology of the P123 aggregates.

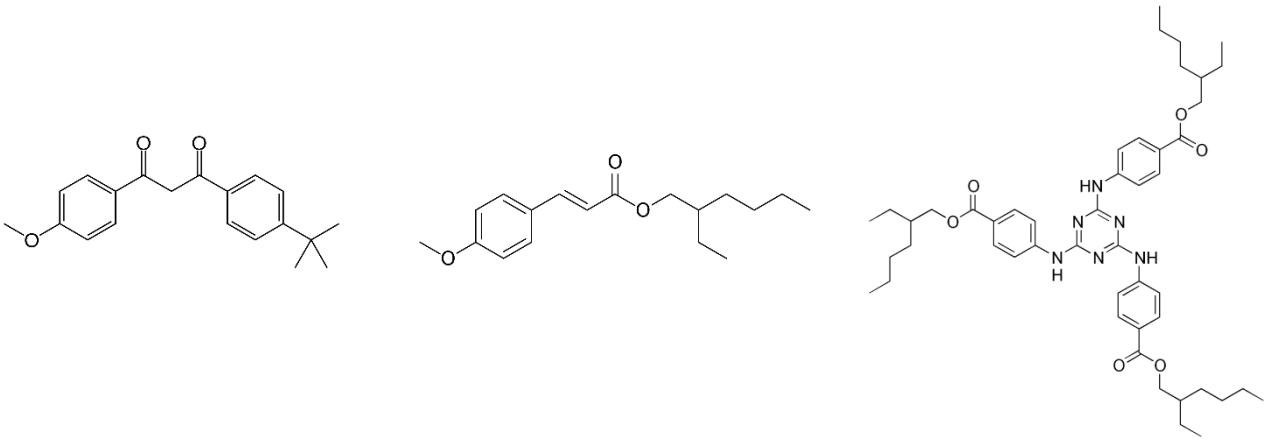

Scheme 1: The chemical structures of Avobenzone (left), Octinoxate (middle) and and Ethylhexyl triazone (right).

2. Materials and Methods

2.1 Materials

The triblock copolymer Pluronic® P123 (EEO_{20}-PPO_{70}-PEO_{20}), average Mn ≈ 5800 g/mol, ethanol (97%), deuterium oxide (D_2O, 99.9%) and 2-ethylhexyl 4-methoxycinnamate (98% purity) were purchased from Sigma Aldrich UK and were used as received. Deuterated ethanol (d_6-anhyrdrous, 99%) was purchased from Goss Scientific UK and was used as received. 1-(4-methoxyphenyl)-3-(4-*tert*-butylphenyl)-1,3-propanedione (Avobenzone, 98% purity), 2,4,6-trianilino(*p*-carbo-2-ethylhexyl-1-oxy)-1,3,5-triazine (Ethylhexyl triazone, 96% purity) were kind gifts from BASF and were used as received.

2.2 Methods

2.2.1 Preparation of Pluronic- UV filters solutions

The different UVA and UVB filters were added to 5 wt% aqueous Pluronic P123 solution containing 10 wt% ethanol (deuterated form for the NMR and SANS measurements). The solutions were left in a HulaMixer for 24 hours at room temperature.

2.2.2 Tensiometry

The surface tension measurements were performed on the samples using a SITA bubble tensiometer (pro line t15, Germany), at 25°C, calibrated by reference to deionised water. To ensure reproducibility, the measurements were repeated five times. The uncertainties in the data were estimated from the minimum and maximum surface tension values recorded.

Nuclear Magnetic Resonance (NMR)

^{1}H NMR spectra were recorded on a JEOL ECZ-600R (600 MHz) at 25 °C, operating at ^{1}H frequency of 600 MHz and equipped with Royal ™ probe 5 mm combined Broadband & Inverse probe and an ACS 64-position sample changer.

2.2.3 Small-angle neutron scattering (SANS)

The SANS experiments were performed on the fixed-geometry, time of flight ZOOM diffractometer (ISIS Spallation Neutron Source, Oxfordshire, UK). The *Q* range explored on ZOOM was between 0.0025–0.5 $Å^{-1}$. The samples were contained in a 1 mm path length, UV-spectrophotometer grade, and quartz cylindrical cuvettes (Hellma). The

cuvettes were mounted in aluminium holders on top of an enclosed, computer-controlled, sample chamber. All measurements were performed at 25°C (± 0.5°C). Temperature control was achieved using a thermostatted circulating bath pumping fluid through the base of the sample changer.

Experimental measuring times were approximately 30 minutes. All scattering data were normalised for the sample transmission and the incident wavelength distribution, corrected for instrumental and sample backgrounds using a quartz cell filled with D_2O (this also removes the instrumental background arising from vacuum windows, *etc.*), and corrected for the linearity and efficiency of the detector response using the instrument specific software package. The data were put onto an absolute scale using a well characterised partially deuterated polystyrene blend standard sample.

2.2.3.1 SANS data analysis

SANS data from Pluronic solutions were fitted using SASview v5.0.4 to a core-shell spherical model [23] or a core-shell cylindrical model[24]. The total volume of the spherical micelles were estimated from:

$$V_{sphere} = \frac{4}{3}\,\pi\,{R_B}^3 \qquad (1)$$

Where R_B is the total radius of the micelle (core + shell), while the total volume of the cylindrical micelle was estimated from:

$$V_{cylinder} = \pi {R_B}^2 h \qquad (2)$$

Where R_B is the total radius of the cylindrical micelle (core + shell), *h* is the overall length of the cylinder. The density number of the micelles could be obtained by dividing the volume fraction of the micelles, Φ_m by the micellar volume (V_{sphere} or $V_{cylinder}$):

$$N_p = \frac{\Phi_m}{V} \qquad (3)$$

The aggregation number (N_{agg}) could be calculated by dividing the volume fraction (Φ_{P123}) of the P123 sample prepared (5%) by the

density number of the micelles, N_p, and the molecular volume (V_{P123}) of one P123 molecule:

$$N_{agg} = \frac{\Phi_{P123}}{N_p V_{P123}} \quad (4)$$

3. Results and Discussion

3.1 Dynamic surface tension (DST)

The DST behaviour from a pure P123 sample at concentrations well above the CMC, Figure 1, shows a gradual decrease in the surface tension values from ≈ 40 $mN.m^{-1}$ to 33 $mN.m^{-1}$ as the bubble life time increases, reaching an equilibrium state at approximately 10 seconds. This is in very good agreement with previous investigations on P123 at different concentrations above the CMC [21, 25].

The DST behaviour from surfactant solutions is sensitive to several factors such as the nature of the surfactant, the chain length, and more importantly here, the presence of any additives. In the pure P123 solution case, the trend in the DST data is consistent with the presence of a significant number of surfactant species, that are available to quickly diffuse and adsorb at the surface of the bubble being introduced in the solution. Goswami *et.al.* discussed the complexity of the interface in the presence of different P123 concentrations, where the different arrangement of the triblock copolymer, in comparison to the non-ionic surfactant $C_{12}E_6$ was found to poorly reflect on the P123 data modelling to the Ward and Tordai model [26].

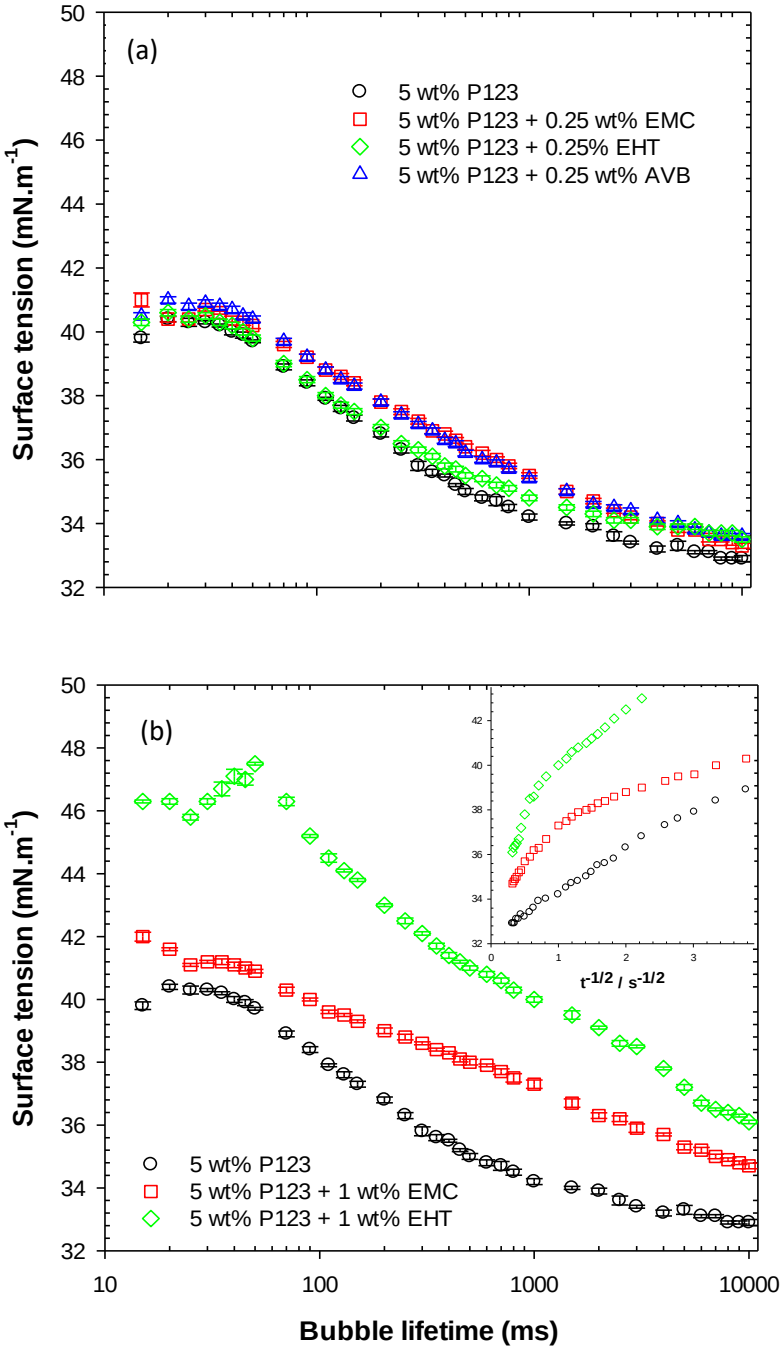

Figure 1: Dynamic surface tension as a function of bubble life time for pure (a) P123 and (b) P123 + UV filter samples, in 10 wt % ethanol in water at 25°C. The inset shows the surface tension *vs.* $t^{-1/2}$ in the same symbols order of the main graph.

As the UV filters are introduced, at relatively low concentrations, 0.25 wt%, we see some changes in the DST behaviour. For example, in the presence of 0.25

wt% EMC, an increase, albeit small, in the surface tension value is observed at the both 'young' and 'old' surface ages, Figure 1. This small increase could be attributed to the low concentrations of the UV filters in the system, especially when comparing it to the 1 wt% case presented later. This overall DST behaviour is indicative of a decrease in the kinetics of the distribution of monomers and micelles. This decrease is presumably attributed to the molecular interactions between the UV filters and the Pluronic molecule, namely the PPO core. The interactions between the hydrophobic salicylic acid molecule and the P123 hydrophobic PPO core have been investigated before by Shah *et.al.* [27], where it was postulated that an increase in the lifetime of the salicylic acid solubilised micelles, led to the disruption of the water molecules around the PPO core. These factors might be expected to also significantly impact the micelle shape and size.

The introduction of the UV filters at higher concentrations, namely EMC and EHT at 1 wt%, has resulted in significant changes in the DST behaviour, namely the slope of the data and the stability of the newly formed interface. The surface tension values at a young surface age (30 ms) in the 1 wt% EHT case for example is ≈ 46 $mN.m^{-1}$(± 0.15), while for the pure P123 sample is ≈ 41 $mN.m^{-1}$ (± 0.09). The lower surface activity exhibited by the P123 + EHT is indeed very interesting. One would expect that the presence of the large hydrophobic UV filter would not lower the surface activity, especially as the aggregation number increases evident by the SANS results (Section 3.3). However, the increase in the size and aggregation number could explain this decrease in surface activity as these larger structures would be slow in migrating to the newly formed interface in bulk [27, 28].

By replotting the tensiometry results to show surface tension vs. $t^{-1/2}$, inset in Figure 1, one is able to highlight the changes in the slopes of the data. By looking at the long times ($t^{-1/2} < 1$), the data is linear which is often related to a diffusion-controlled process. However, it should be noted that drawing further conclusions from this representation is limited by the large molecular size of the Pluronic P123, and how it could change its configuration at the air-water interface. The magnitude of these slopes has been previously linked to the surfactant's hydrophobicity in a given environment, *i.e.*, the steeper the slope, the higher the hydrophobicity[29, 30], which in our case could be

attributed to the variation in the size of the P123 micelles in the presence of the various UV filters.

3.2 Nuclear magnetic resonance (NMR)

Our NMR data further highlight the interactions between P123 and the UV filters (for reference, full width NMR spectra from the UV filters and P123 have been included in the electronic supporting information, Figures 1S-4S). The peaks from the P123 + EHT sample (red line, Figure 2) at ≈ 1.0 ppm from the PO-CH_3 group and at ≈ 3.5 – 3.2 ppm from the PO-CH_2 have shown a change in their position and width, pointing towards the presence of strong molecular interactions between the PPO groups and EHT. The upfield shift of the peaks from the mixture strongly points to the creation of a further hydrophobic environment at the PPO core. In comparison, the peak from the EO-CH_2 group at ≈ 3.6 ppm shows little change in its width and chemical shift, indicative of weaker interactions between EHT and this group where it remains in contact with water.

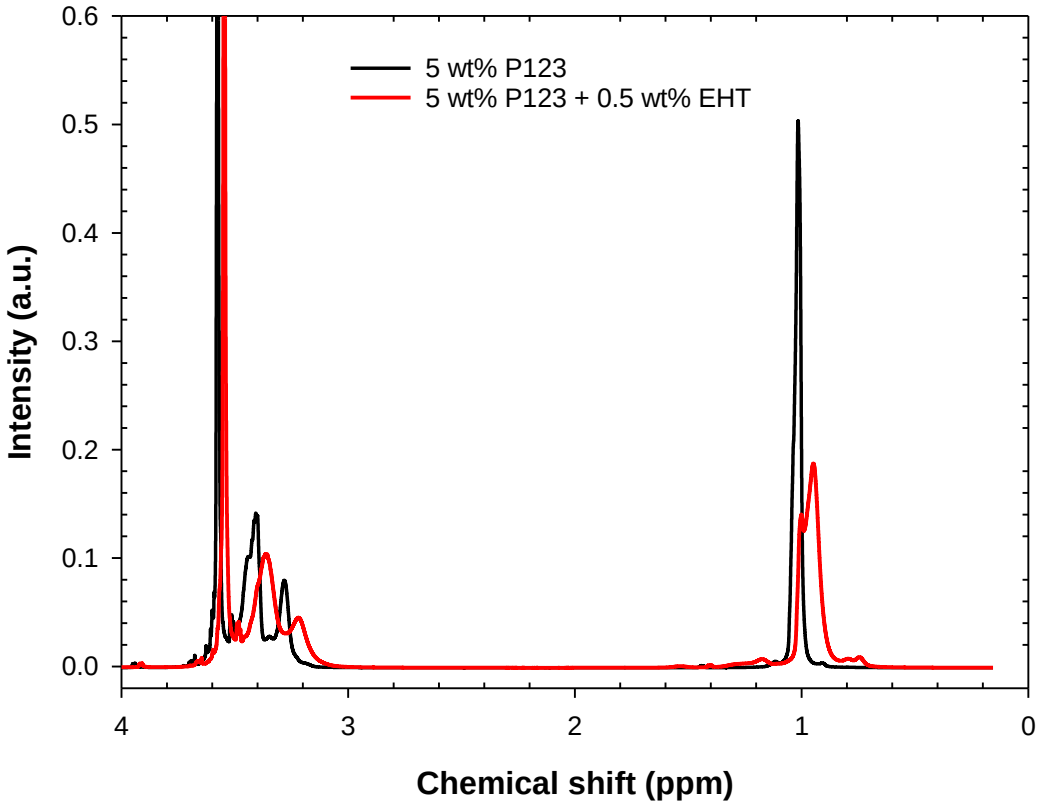

Figure 2: ^{1}H NMR spectra from P123 (black) and P123 + EHT (red) in 10 wt% d_6-ethanol and D_2O.

Generally, the NMR data also present these strong interactions through sharp changes in the aromatic peaks from the UV filters at the ≈ 8.0 – 6.0 ppm range. The example presented here, Figure 3, is from a sample comprising P123 and EMC. The spectra show that the intensity of the EMC aromatic peaks in the presence of the P123 micelles has become weaker and that the peaks have become broader. The effect of the EMC on the chemical shift of the P123 PO-CH_2, PO-CH_3 and the EO-CH_2 chemical groups is also shown, Figure 5S. A short T_2 relaxation time is likely behind these changes in the peaks' resolution.

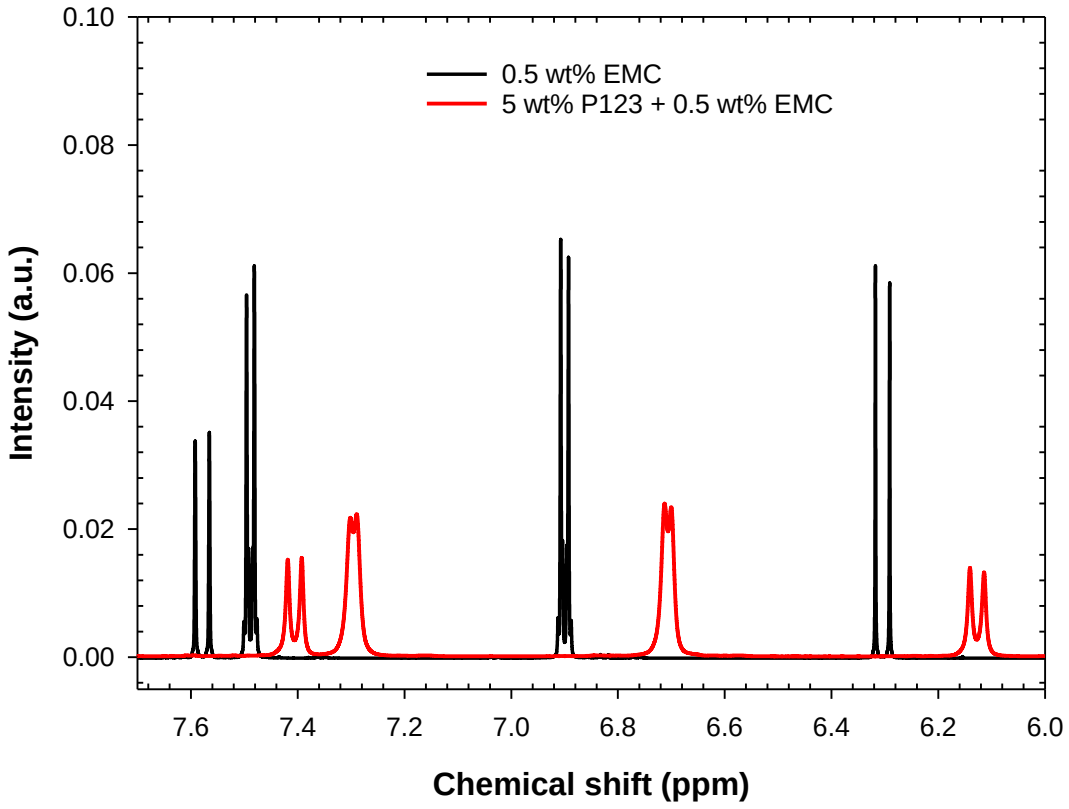

Figure 3: ^{1}H NMR spectra from EMC (black) in d_6-ethanol and P123 + EMC (red) in 10 wt% d_6-ethanol and D_2O.

If one is to hypothesise, based on the spectra, that the EMC is interacting with both the PPO and the PEO groups, this would mean that a percentage of the EMC is present at the palisade of the micelle. As a result, this would cause

some broadening in the NMR signal, as there will be a quick relaxation (in comparison to the time of the experiment) of the NMR resonance from the aromatic group present at this area as noted above. This broadening in the signal could be further highlighted by the NMR spectra from samples comprising EHT/EHT + P123 and AVB/AVB+P123, Figure 6S and 7S.

3.3 Small-angle neutron scattering (SANS)

In this section we examine the effect of the three UV filters, at different concentrations, on the Pluronic P123 micelle structure. First, we investigate the effect of EMC at three different concentrations, 0.1, 0.5 and 1 wt%, Figure 4. SANS from Pluronic P123 micelles has been reported before [21, 31], where in general, core shell spherical micelles were observed. Similar structures were present here, evident by a peak or a 'bump' in the data at ≈ 0.09 $Å^{-1}$ (d≈ 69 Å), corresponding to a well-defined core shell structure.

Our data fitting to the core-shell model as discussed in section 2.2, showed the presence of these aggregates with a core radius of ≈ 49 Å, shell thickness of ≈ 11 Å and an aggregation number of 50, Table 1, in good agreement with previously published work from P123 solutions containing ethanol [14, 25]. It must be noted though that a limitation of this method estimating the aggregation number is that it does not consider the degree of hydration of the PEO in the micelle's shell and its effect on the thickness of the shell. The data fitting routine to the core-shell model however provides information to the sensitivity of both the radius of the core and the shell thickness. We estimate a relative error of ≈ 5% on the aggregation number as the accuracy on both terms is 1 Å, Tables I and II. The introduction of low concentrations of EMC, namely 0.1 wt%, has resulted in an increase of the volume of the core-shell micelle from 900 nm^3 to 1200 nm^3. This strongly points to the preferential solubilisation of the EMC by the P123, also evident from the NMR results as reported earlier. A significant shift in the position of the bump at mid Q towards low Q is observed in the presence of 0.5 wt% EMC, where now an overall radius (core + shell) of ≈ 75 Å was obtained from the data modelling, in comparison to ≈ 60 Å from the pure micelles. This increase could also be extended to the micellar volume and the aggregation number calculated from this sample, Table 1. Spherical core-shell

micelles were also observed in mixtures of P123 and the AVB molecule, Figure 2S, where similar conclusions to the P123 + EMC system (based on the scattering behaviour and fittings parameters, Table 1S) could be drawn. These similarities could be attributed to their molecular weight and more importantly, their *log P* values[32, 33].

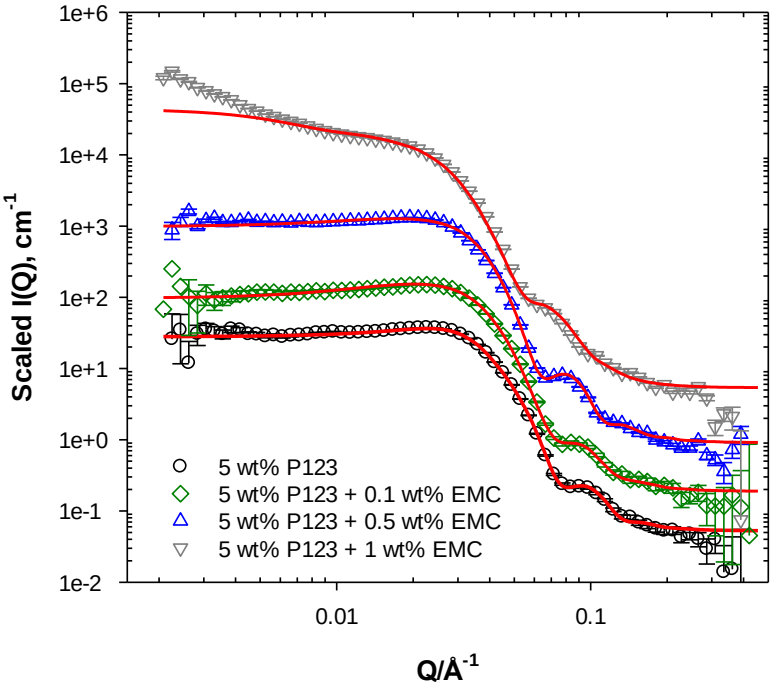

Figure 4: SANS from P123 micelles and P123 micelles + EMC at different concentrations, at 25°C in 10 wt% d_6-ethanol and D_2O. Data has been staggered for clarity. Solid lines correspond to fits to core-shell spheres (0.1 wt%, 0.5 wt% EMC) and core-shell cylinders (1 wt% EMC).

EMC concentration (wt%)	**0**	**0.1**	**0.5**	**1**
Core radius, Å (±1)	49	51	60	59
Shell thickness, Å (±1)	11	15	14	11
Length, Å ± (5)	-	--	--	800
Volume fraction	0.1	0.11	0.11	0.095
Volume of the micelle (nm^3)	904	1205	1700	12700
Number density of micelles, 10^{-17} (cm^{-3})	1.1	0.9	0.6	0.07
Aggregation number	50 ± 2.5	61 ± 3.0	85 ± 4.2	735 ± 36.7

Table I: SANS fitting parameters from P123 micelles (5 wt%) and EMC at different concentrations, in 10 wt% d_6-ethanol and D_2O, at 25°C.

The most significant impact on the P123 micelle could be observed in the presence of 1 wt% EMC. The data features a Q^{-2} slope at low Q, indicative of a cylindrical structure, in addition to a bump at ≈ 0.065 Å, suggesting it also is a well-defined core-shell cylinder. This is indeed also evident from our data modelling, where a core-shell cylinder model revealed a cylinder length of 800 Å and an aggregation number of 735. The large size of these cylinders has also resulted in a significant decrease in the number density micelles, Table 1. The modelling however does not seem to capture some of the data at low Q. This is most likely due to aggregation of the micelles at that particular length scale.

The transition from spherical to cylindrical micelles is most likely attributed to the high concentration of the EMC rather than its presence only, as an increase in the spherical micelle size was also observed at lower EMC concentrations. The introduction of 1 wt% EMC to the micelle, and its interaction with both the PEO shell and the PPO core as evident from the NMR spectra, could mean that the EMC has resulted in a core and/or shell dehydration, prompting the micellar transition.

Sphere to cylinder transition in Pluronic aggregates was previously reported by Shah *et.al*. where the presence of salicylic acid was found to cause core dehydration, resulting in the structural transition [27]. Pluronic P85 spherical micelles transition to cylindrical ones was also reported as a result of shell dehydration by Parekh *et.al.* [34] However, it is not yet clear which of the two dehydration processes is the main driving force behind this transition. This is also further complicated when the hydrophobic molecule is solubilised within the Pluronic micelle interacting with both PPO and PEO.

On the other hand, the introduction of the larger EHT molecule to the P123 micelles has resulted in changes in its aggregation and scattering behaviour, Figure 5. However, we must note that the degree of change does not correlate to the EHT molecular size and concentration. This is further clarified by comparing the effect of the EMC and the EHT on the P123 micelle. For example, at 0.5 wt% EHT, the SANS fitting routine, Table 2, reveals a

spherical core-shell micelle with an overall radius of ≈ 72 Å - largely similar to the P123 + EMC profiles. Furthermore, if the EHT has promoted the presence of more micelles rather than increase its size, one would expect a significant increase in the number density of micelles, as well as an increase in the I(Q) in the unstaggered data, Figure 9S and 10S, however that is not the case here, where both terms remain very similar to the ones obtained from the P123 + EMC micelles.

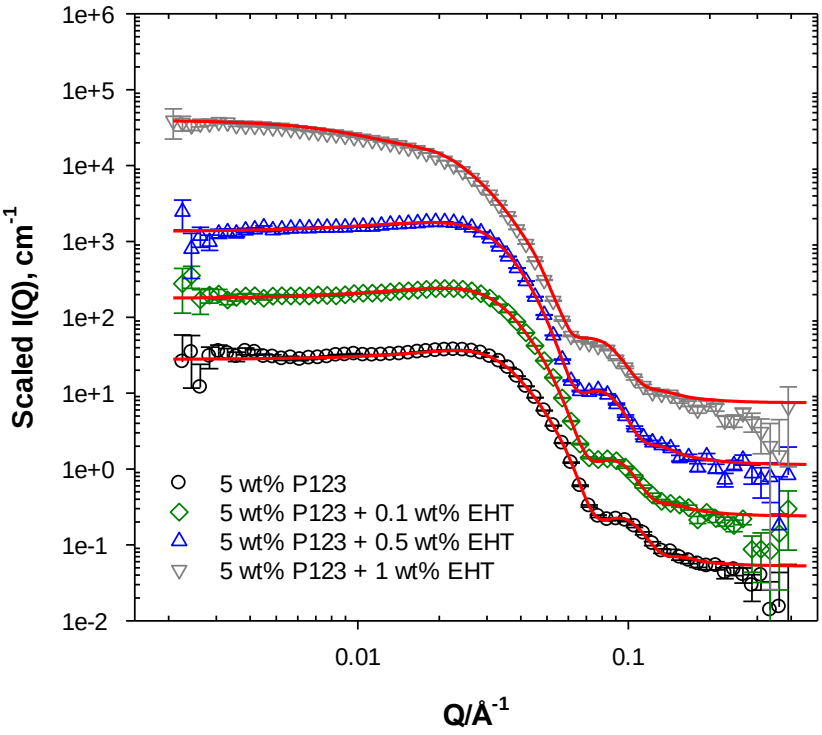

Figure 5: SANS from P123 micelles and P123 micelles + EHT at different concentrations, at 25°C in 10 wt% d_6-ethanol and D_2O. Data has been staggered for clarity. Solid lines correspond to fits to core-shell spheres (0.1 wt%, 0.5 wt% EHT) and core-shell cylinders (1 wt% EHT).

EHT concentration (wt%)	0	0.1	0.5	1
Core radius, Å (±1)	49.2	53	59	53
Shell thickness, Å (±1)	11.4	13	13	14
Length, Å (± 5)	-	-	--	500
Volume fraction	0.1	0.11	0.11	0.095
Volume of the micelle (nm^3)	904	1208	1563	7051
Number density of micelles, 10^{-17} (cm^{-3})	1.1	0.9	0.7	0.1
Aggregation number	50 ± 2.5	60 ± 3.0	78 ± 3.9	432 ± 21.6

Table II: SANS fitting parameters from P123 micelles (5 wt%) and EHT at different concentrations, in 10 wt% d_6-ethanol and D_2O, at 25°C.

The similarity in the aggregation behaviour between the P123/EMC, and P123 /EHT systems strongly suggests weaker interactions between the P123 micelles and the EHT. This could be explained by a preferential interaction between EHT and EO and PO in solution, in addition to the solubilisation by the Pluronic micelle- the hydrotope effect. Nguyen-Kim *et.al.* have investigated the interactions between carbamazepine, fenofibrate and a range of Pluronic®, where weaker interactions between Pluronic and carbamazepine were noted, evidenced by no significant changes in the micellar size. It was noted that in this case, the Pluronic® acted as a double agent, once as a micellar solubiliser, and also as a hydrotope [35].

4. Conclusions

By combining tensiometry, NMR and SANS, we were able to investigate the effect of three commonly used organic UV filters; AVB, EMC and EHT, at different concentrations, on the micellar properties of Pluronic® P123. First, the introduction of the UV filters to the P123 micelles has resulted in high dynamic surface tension values, strongly suggesting that larger aggregates, with reduced availability of free monomers, are present in bulk. NMR has allowed us to probe the molecular interactions between the UV filters and P123, where the strongest interactions were observed between the core PPO groups and the

UV filters. This was followed by the shell PEO groups and the UV filters, suggesting that the UV filter is indeed present at both the core and the palisade of the micelle. Future work involving 2D NMR techniques such as PGSE-NMR would be beneficial as it would allow us to quantify the partitioning of the UV filters across the micelle. The findings from the SANS measurements could allow us to postulate that: (a) spherical to cylindrical transitions are present in these systems, triggered by the UV filter and its concentration, (b) preferential solubilisation of the UV filters in the P123 core and (c) the significant increase in the size of the hydrophobic UV filter molecule does not necessarily translate to an equally significant increase in the micellar size, as evident in the EHT case, where the hydrotope effect might be present. These results provide insights for formulators utilising the many benefits of Pluronic® triblock copolymers in sun protection formulations, highlighting the sensitivity of these materials to the presence of UV filters, and the subsequent effects it could have on the latter's accessibility and performance. This could be evaluated in the future using ISO approved *in vitro* SPF measurements and skin permeation studies.

Declaration of Competing interests

The authors declare that they have no known competing financial interests or personal relationships that could have appeared to influence the work reported in this paper.

References

[1] Tampucci S, Burgalassi S, Chetoni P, et al. Cutaneous permeation and penetration of sunscreens: Formulation strategies and in vitro methods. *Cosmetics* 2018; 5: 1.

[2] Yoon MS, Chung YB, Han K. A study of gel structure in the nonionic surfactant/cetostearyl alcohol/water ternary systems by differential scanning calorimeter. *J Dispers Sci Technol* 1999; 20: 1695–1713.

[3] da Silva Souza ID, Berkowitz E, Chea JD, et al. Efficient UV Filter Solubilizers Prevent Recrystallization Favoring Accurate and Safe Sun Protection. *ACS Appl Mater Interfaces* 2018; 10: 40411–40423.

[4] Newlands C, Currie R, Memon A, et al. Non-melanoma skin cancer: United Kingdom National Multidisciplinary Guidelines. *J Laryngol Otol* 2016; 130: S125–S132.

[5] Griffin LL, Faisal A, Ali R, et al. Non-melanoma skin cancer. *CME DERMATOLOGY Clinical Medicine* 2016; 16: 62–67.

[6] Alexandridis P, Hatton TA. Block copolymer surfactants in aqueous solutions and at interface: thermodynamics, structure, dynamics and modeling. *Colloids Surf A Physicochem Eng Asp* 1995; 96: 1–46.

[7] Tănase MA, Raducan A, Petru¸ta Oancea P, et al. Mixed Pluronic-Cremophor Polymeric Micelles as Nanocarriers for Poorly Soluble Antibiotics-The Influence on the Antibacterial Activity. *Pharmaceutics* 2021; 13: 435.

[8] Han Y, Zhang Z, Smith GS, et al. Effect of nucleoside analogue antimetabolites on the structure of PEO-PPO-PEO micelles investigated by SANS. *Physical Chemistry Chemical Physics* 2017; 19: 15686–15692.

[9] Valero M, Hu W, Houston JE, et al. Solubilisation of salicylate in F127 micelles: Effect of pH and temperature on morphology and interactions with cyclodextrin. *J Mol Liq* 2021; 322: 114892.

[10] Powell KC, Damitz R, Chauhan A. Relating emulsion stability to interfacial properties for pharmaceutical emulsions stabilized by Pluronic F68 surfactant. *Int J Pharm* 2017; 521: 8–18.

[11] Leister N, Karbstein HP. Influence of hydrophilic surfactants on the W1-W2 coalescence in double emulsion systems investigated by single droplet experiments. *Colloids and Interfaces* 2021; 5: 21.

[12] Kathe K, Kathpalia H. Film forming systems for topical and transdermal drug delivery. *Asian Journal of Pharmaceutical Sciences* 2017; 12: 487–497.

[13] Newby GE, Hamley IW, King SM, et al. Structure, rheology and shear alignment of Pluronic block copolymer mixtures. *J Colloid Interface Sci* 2009; 329: 54–61.

[14] Mansour OT, Cattoz B, Heenan RK, et al. Probing competitive interactions in quaternary formulations. *J Colloid Interface Sci* 2015; 454: 35–43.

[15] Hanson KM, Cutuli M, Rivas T, et al. Effects of solvent and micellar encapsulation on the photostability of avobenzone. *Photochemical and Photobiological Sciences* 2020; 19: 390–398.

[16] Hanno I, Centini M, Anselmi C, et al. Green cosmetic surfactant from rice: Characterization and application. *Cosmetics* 2015; 2: 322–341.

[17] Gaspar LR, Maia Campos PMBG. Rheological behavior and the SPF of sunscreens. *Int J Pharm* 2003; 250: 35–44.

[18] Hanno I, Centini M, Anselmi C, et al. Green cosmetic surfactant from rice: Characterization and application. *Cosmetics* 2015; 2: 322–341.

[19] Liu W, Wang X, Lai W, et al. Sunburn protection as a function of sunscreen application thickness differs between high and low SPFs. *Photodermatol Photoimmunol Photomed* 2012; 28: 120–126.

[20] Grillo I, Morfin I. Structural characterization of Pluronic micelles swollen with perfume molecules. *Langmuir* 2018; 34: 13395–13408.

[21] Alexander S, Cosgrove T, Castle TC, et al. Effect of Temperature , Cosolvent , and Added Drug on Pluronic − Flurbiprofen Micellization. *J Phys Chem B* 2012; 116: 11545–11551.

[22] Couteau C, Philippe A, Ali A, et al. Study of the influence of alcohol on the photostability of four UV filters. *Eur Rev Med Pharmacol Sci* 2021; 25: 6025–6033.

[23] Hammouda B. SANS from Pluronic P85 in d-water. *Eur Polym J* 2010; 46: 2275–2281.

[24] Kline SR. Reduction and analysis of SANS and USANS data using IGOR Pro. *J Appl Crystallogr* 2006; 39: 895–900.

[25] Jangher A, Griffiths PC, Paul A, et al. Polymeric micelle disruption by cosolvents and anionic surfactants. *Colloids Surf A Physicochem Eng Asp* 2011; 391: 88–94.

[26] Goswami A, Verma G, Hassan PA, et al. Equilibrium and Dynamic Surface Tension Behavior of Triblock Copolymer PEO-PPO-PEO in Aqueous Medium. *J Dispers Sci Technol* 2015; 36: 885–891.

[27] Shah V, Bharatiya B, Patel V, et al. Interaction of salicylic acid analogues with Pluronic® micelles: Investigations on micellar growth and morphological transition. *J Mol Liq* 2019; 277: 563–570.

[28] Kanokkarn P, Shiina T, Santikunaporn M, et al. Equilibrium and dynamic surface tension in relation to diffusivity and foaming properties: Effects of surfactant type and structure. *Colloids Surf A Physicochem Eng Asp* 2017; 524: 135–142.

[29] Gao T, Rosen MJ. Dynamic Surface Tension of Aqueous Surfactant Solutions: 7. Physical Significance of Dynamic Parameters and the Induction Period. *J Colloid Interface Sci* 1995; 172: 242–248.

[30] Wang X-C, Zhang L, Gong Q-T, et al. Study on Foaming Properties and Dynamic Surface Tension of Sodium Branched-alkyl Benzene Sulfonates. *J Dispers Sci Technol* 2009; 30: 137–143.

[31] Foster B, Cosgrove T, Hammouda B. Pluronic triblock copolymer systems and their interactions with ibuprofen. *Langmuir* 2009; 25: 6760–6766.

[32] Tampucci S, Burgalassi S, Chetoni P, et al. Cutaneous permeation and penetration of sunscreens: Formulation strategies and in vitro methods. *Cosmetics*; 5. Epub ahead of print 1 March 2018. DOI: 10.3390/cosmetics5010001.

[33] Wang SQ, Osterwalder U, Jung K. Ex vivo evaluation of radical sun protection factor in popular sunscreens with antioxidants. *J Am Acad Dermatol* 2011; 65: 525–530.

[34] Parekh P, Ganguly R, Aswal VK, et al. Room temperature sphere-to-rod growth of Pluronic® P85 micelles induced by salicylic acid. *Soft Matter* 2012; 8: 5864–5872.

[35] Nguyen-Kim V, Prévost S, Seidel K, et al. Solubilization of active ingredients of different polarity in Pluronic® micellar solutions - Correlations between

solubilizate polarity and solubilization site. *J Colloid Interface Sci* 2016; 477: 94–102.